

Hanle effect near boundaries: Diffusion-induced lineshape inhomogeneity

Hans-Andreas Engel

Department of Physics, Harvard University, Cambridge, Massachusetts 02138, USA

(Received 25 July 2007; published 4 March 2008)

The Hanle effect describes suppression of spin polarization due to precession in a magnetic field. This is a standard spintronics tool and it gives access to the spin lifetime of samples in which spins are generated homogeneously. We examine the Hanle effect when spins are generated at a boundary of a diffusive sample by the extrinsic spin Hall effect. We show that the Hanle curve is spatially dependent and that the “apparent” spin lifetime, given by its inverse half-width, is shorter near the boundary even if the spin relaxation rate is homogeneous.

DOI: [10.1103/PhysRevB.77.125302](https://doi.org/10.1103/PhysRevB.77.125302)

PACS number(s): 72.25.Rb, 72.25.Dc, 72.25.Fe

I. INTRODUCTION

The goal of spintronics is to generate and manipulate spin populations on time scales limited by the spin lifetime. One can access the spin population optically, since selection rules allow optical pumping and detection of spins in materials;¹ interesting alternatives are magnetic materials or materials with spin-orbit interaction, providing access to spins with standard microelectronic devices.^{2,3} To characterize a given sample, it is essential to determine its spin lifetime τ_s , which depends on the microscopic properties of the sample. One can determine τ_s of a homogeneous sample using the Hanle effect¹ as follows, even if time-resolved measurements are not available. If there is no spin precession, a spin polarization simply decays with the spin relaxation rate $1/\tau_s$. However, if a magnetic field B perpendicular to the spin polarization axis is applied, there is a competing relaxation mechanism: Spins will precess in that magnetic field with Larmor frequency $\omega_L \propto B$. If the magnetic field is sufficiently large, such that the spin can precess many times within its lifetime, this will randomize the spin and suppress the spin polarization. This competing spin relaxation mechanism becomes effective for $\omega_L \gtrsim 1/\tau_s$; thus τ_s can be extracted by measuring the inverse width of the so-called Hanle curve $s_z(\omega_L)$.

In recent experiments by Kato *et al.*,⁴ a spatially dependent spin polarization s_z was induced via the extrinsic spin Hall effect^{5–8} and measured via Kerr microscopy. The width of the Hanle curves $s_z(\omega_L, \mathbf{r})$ was described with a spatially dependent spin lifetime $\tilde{\tau}_s(\mathbf{r})$. Rather strikingly, it was found that $\tilde{\tau}_s$ is several times smaller near the sample edge than 10 μm away from the edge. In this paper, we calculate the Hanle curves and show that such a suppression of $\tilde{\tau}_s$ near the edge can result from spin diffusion, even if the spin relaxation rate τ_s^{-1} is spatially *homogeneous*.

The physical picture for this spatial dependence of $\tilde{\tau}_s$ is as follows [see Figs. 1(a) and 1(b)]. Spins are generated at the boundary and then diffuse into the bulk of the sample. In a magnetic field, the spins observed at a small distance x were (on average) generated a short time ago and did not yet precess much in the magnetic field. Therefore, they have a larger s_z than one would expect for the homogeneous case with a bulk generation mechanism (e.g., optical pumping). This means that the linewidth as function of B is larger and

the spin lifetime seems smaller. Conversely, the spins observed far from the boundary required a rather long time to get there and were able to precess longer in the magnetic field. Therefore, the value of s_z is more strongly suppressed by B , the linewidth becomes narrower, and the spin lifetime appears longer.

A similar situation is found when the dominating spin transport mechanism is the drift induced by charge currents.^{9–12} During the drift from the injection to the detection point over a distance r , spins precess during time $t = r/v_{\text{dr}}$, where v_{dr} is the drift velocity. Because the precession angle $\omega_L t$ is the same for each spin (neglecting diffusion),

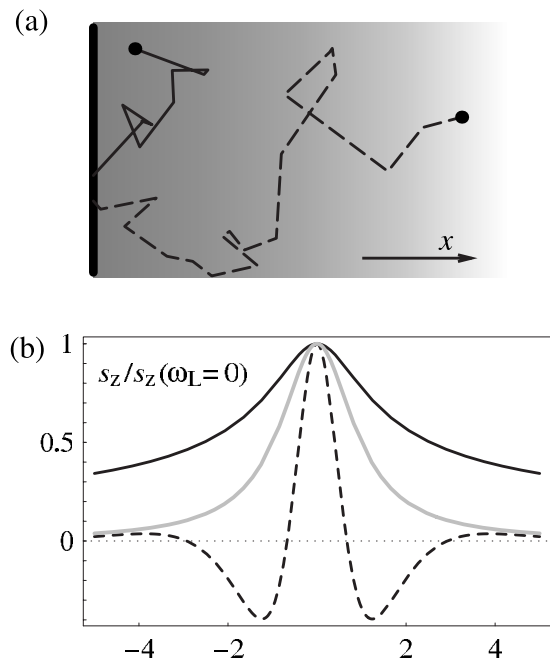


FIG. 1. (a) When spins are generated at the boundary and then diffuse into the sample, spins closer to the boundary had, on average, less time to precess in the magnetic field $\mathbf{B} = B\hat{x}$ than those further away. (b) Therefore, the Hanle curve $s_z(\omega_L \propto B)$ close to the boundary ($x=0$, solid line) becomes broader, while away from the boundary ($x=4L_s$ with spin diffusion length L_s , dashed line), it becomes narrower than in the case of homogeneous spin generation (gray line). Here, the spin density $s_z(x, \omega_L)$ is given by Eq. (6) for $\tau_s = \tau_{xy} = \tau_z$ and $q_s = 0$.

multiple oscillations of s_z were observed as function of ω_L (Ref. 9) or r .¹⁰

II. MODEL

To quantitatively describe the suppression of the apparent spin lifetime $\tilde{\tau}_s$ in a diffusive system, we now analyze the Hanle curves for such systems. For this, we consider a magnetic field $\mathbf{B} = B\hat{x}$, which induces spin precession of electrons with Larmor frequency $\omega_L = g^* \mu_B B / \hbar$, with effective g factor g^* and Bohr magneton μ_B , corresponding to a Zeeman coupling $H_Z = \frac{1}{2} g^* \mu_B \mathbf{B} \cdot \boldsymbol{\sigma}$. We assume a sufficiently small magnetic field that orbital effects are not important and that $\tilde{\tau}_s^{-1}$ is independent of B . The equation of motion for the spin density \mathbf{s} , including spin precession, diffusion, and relaxation, is

$$\dot{\mathbf{s}} = (g^* \mu_B / \hbar) \mathbf{B} \times \mathbf{s} + D \Delta \mathbf{s} - \tilde{\tau}_s^{-1} \mathbf{s}, \quad (1)$$

with a spatially independent spin diffusion constant D and a diagonal spin relaxation tensor $\tilde{\tau}_s^{-1}$ with components $\{\tau_{xy}^{-1}, \tau_{xy}^{-1}, \tau_z^{-1}\}$; note that the polarization s_x decouples and so its spin relaxation rate is actually not important here. Also, we define the geometrical mean of the spin relaxation times as $\tau_s = \sqrt{\tau_{xy} \tau_z}$ and the spin diffusion length is $L_s = \sqrt{D \tau_s}$. We set $\tau_{xy} = \alpha \tau_s$ and $\tau_z = \alpha^{-1} \tau_s$ with some dimensionless constant α , e.g., $\alpha = \sqrt{2}$ for Dyakonov-Perel spin relaxation and Rashba coupling.^{13–16}

Next, we assume that spin polarization is generated at a boundary plane. This is the case for the extrinsic spin Hall effect,^{4–8} where a (homogeneous) electrical current induces spin currents which, in turn, produce spin polarization near sample edges due to extrinsic spin-orbit interaction. We take a semi-infinite two- or three-dimensional system with $x \geq 0$ and an electric field E_y applied along the y direction. The transverse spin current is $j_x^z = \sigma_{\text{SH}} E_y$, with spin Hall conductivity σ_{SH} . Microscopically, the spin current relaxes on the short transport lifetime $\tau \ll 1 / \omega_L$; thus, σ_{SH} does not depend on the weak magnetic field. If spin is conserved at the boundary, there is no spin current perpendicular to the boundary and the spin Hall current is compensated by spin diffusion, i.e., $j_x^z = D \frac{\partial}{\partial x} s_z$ at $x=0$. More generally, we consider the boundary condition

$$\frac{\partial}{\partial x} s_z = \frac{j_x^z}{D} + q_s s_z, \quad \frac{\partial}{\partial x} s_y = q_s s_y, \quad (2)$$

which allows for spin relaxation at the edge, characterized by q_s , and where we have taken $j_x^y = 0$. Note that the spin relaxation described by q_s occurs on length scales much shorter than L_s .^{17,18}

A. Comparison to other systems

For other systems, where spins are generated at a boundary and then precess in a field, Eqs. (1) and (2) also apply and these systems show the same Hanle curves. D'yakonov and Perel¹⁹ considered the situation where electron spins were optically generated using circularly polarized light in a surface layer thinner than L_s . Assuming that recombination only takes place in this surface layer, it is taken into account

via q_s . Further, the degree of circular polarization of the recombination radiation is proportional to s_z at $x=0$, so only the Hanle curve at the surface is experimentally accessible. Such measurements were reported by Vekua *et al.*²⁰ Furthermore, Johnson and Silsbee²¹ analyzed a system where spins are injected from a ferromagnet into a paramagnet at $x=0$. A second ferromagnet at a distance x is used as a detector, whose voltage is proportional to the spin polarization $s_z(x)$. Fabrication of devices with different detector spacings then provides electrical access to the spatially dependent Hanle curve.

B. Hanle curves

We now analyze the spin polarization in the stationary case $\dot{\mathbf{s}}=0$ by assuming that the spin relaxation rate $\tilde{\tau}_s^{-1}$ is *spatially independent*. With the ansatz $\mathbf{s} = \mathbf{s}_0 e^{q x}$, we find the solutions of Eq. (1) satisfying $\text{Re } q < 0$, with wave numbers

$$q_{0,1} = - \sqrt{\frac{\tau_{xy} + \tau_z \pm T}{2D \tau_{xy} \tau_z}}, \quad (3)$$

$$T = \sqrt{(\tau_{xy} - \tau_z)^2 - 4 \tau_{xy}^2 \tau_z^2 \omega_L^2}, \quad (4)$$

and we have defined T for later convenience. From the boundary conditions (2), we obtain the position-dependent Hanle curves

$$s_y(x, B) = j_x^z \sum_{i=0,1} e^{q_i x} \frac{(-1)^i \tau_{xy} \tau_z \omega_L}{DT(q_i - q_s)}, \quad (5)$$

$$s_z(x, B) = j_x^z \sum_{i=0,1} e^{q_i x} \frac{T + (-1)^i (\tau_{xy} - \tau_z)}{2DT(q_i - q_s)}. \quad (6)$$

For $\tau_{xy} = \tau_z = \tau_s$, Eq. (6) simplifies considerably; using $q_{0,1} L_s = -\sqrt{1 \pm i \omega_L \tau_s} = -(\kappa_R \pm i \kappa_I)$ with $\kappa_R = (1 + \sqrt{1 + \omega_L^2 \tau_s^2})^{1/2} / \sqrt{2}$ and $\kappa_I = \omega_L \tau_s / 2 \kappa_R$, we find

$$s_z(d) = - \frac{j_x^z \sqrt{\tau_s} [(\kappa_R + \beta) \cos \kappa_I d + \kappa_I \sin \kappa_I d]}{\sqrt{D} [(\kappa_R + \beta)^2 + \kappa_I^2]} e^{-\kappa_R d}, \quad (7)$$

where we have defined the dimensionless distance $d = x / L_s$ and the dimensionless boundary relaxation $\beta = q_s L_s$ (Fig. 2). In the special case of $x=0$ and $\tau_{xy} = \tau_z$, Eq. (7) agrees with the expression found when studying Hanle effect on surfaces,^{19,20} while for $q_s=0$ and $\tau_{xy} = \tau_z$, it agrees with the result from Ref. 21.

Further, in the absence of the magnetic field, Eq. (6) simplifies to $s_z = -j_x^z \sqrt{\tau_s} / D e^{-\sqrt{\alpha} x / L_s} / (\sqrt{\alpha} + \beta)$. Finally, for $q_s=0$, the integrated spin density corresponds to the Hanle curve of a homogeneous system,

$$\int dx s_z(x) = - \frac{j_x^z \tau_z}{1 + \tau_s^2 \omega_L^2}. \quad (8)$$

C. Apparent spin lifetime

In the experiments of Ref. 4 the apparent spin lifetime $\tilde{\tau}_s(x)$ is extracted by assuming a Lorentzian Hanle curve [Eq.

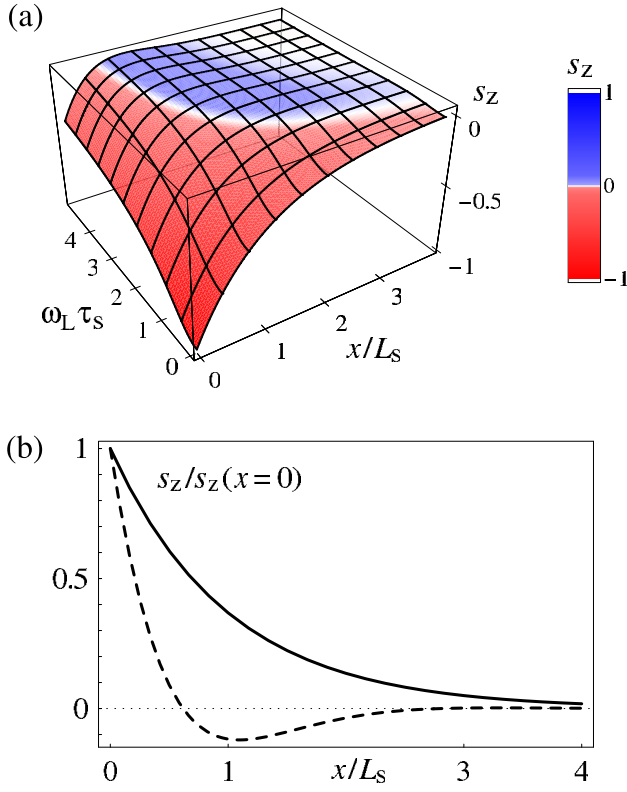


FIG. 2. (Color online) [(a) and (b)] Spin density $s_z(x, \omega_L)$ near a boundary of a diffusive system, given by Eq. (6) for $\tau_s = \tau_{xy} = \tau_z$ and $q_s = 0$. Sufficiently far from the boundary, the Hanle curve develops side lobes (Refs. 21 and 22) where the spin polarization changes sign; here, s_z is plotted in units of $j_x^z \sqrt{\tau_s}/D$. (c) Spins generated at the boundary diffuse into the sample in the absence of a magnetic field and eventually become suppressed due to spin relaxation ($\omega_L = 0$, solid line), while in a magnetic field ($\omega_L = 5\tau_s^{-1}$, dashed line), spin precession further suppresses spin polarization.

(8)] at each position, then τ_s can be found as the half-width at half maximum of $s_z(\omega_L)$. Correspondingly, we now take Eq. (6) and solve $\frac{1}{2}s_z(x, \omega_L=0) = s_z(x, \omega_L^{\text{HWHM}})$ for the apparent spin lifetime $\tilde{\tau}_s(x) = 1/\omega_L^{\text{HWHM}}$. Since $\tilde{\tau}_s$ does not depend on the prefactor j_x^z in s_z , it is a function of α , β , τ_s , x , and D . From dimensional analysis, we see that

$$\tilde{\tau}_s = \tau_s g_{\alpha, \beta} \left(\frac{x}{L_s} \right), \quad (9)$$

with some dimensionless function $g_{\alpha, \beta}$ that depends on the distance $d = x/L_s$ from the boundary in units of the spin diffusion length.

Using Eq. (6), we evaluate $g_{\alpha, \beta}(d)$ numerically and plot it in Fig. 3. For example, $g_{1,0} \approx 0.43 + 0.52d$ within 5% and for $d < 10$. Most importantly, the “apparent” spin relaxation time $\tilde{\tau}_s$ shows a strong spatial dependence, even if the underlying spin relaxation rate is homogeneous. In particular, this means that $\tilde{\tau}_s$ is roughly *four times smaller* near the boundary than several (three to four) spin diffusion lengths away. This is in agreement with the experiments^{4,11,23} where a similar factor was observed.²⁴

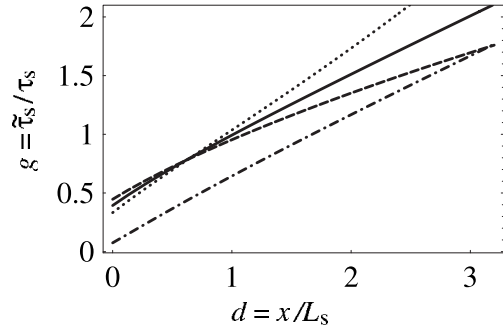


FIG. 3. Apparent spin relaxation time $\tilde{\tau}_s$ as function of distance x from boundary, plotted for $\beta=0$ and $\alpha=1$ (solid line), $\alpha=\sqrt{2}$ (dashed), $\alpha=1/\sqrt{2}$ (dotted) and for $\beta=2$ and $\alpha=1$ (dashed-dotted). While details depend on the microscopic parameters (see text), generally, the apparent spin lifetime is reduced when considering the Hanle curves close to the boundary, even if the spin relaxation rate is position independent.

III. DISCUSSION

An important question is what happens at the boundary of a homogeneous sample, namely, if there are spin relaxations processes due to the boundary. Such processes, on length scales shorter than L_s , are included here via q_s . By measuring the spatially dependent Hanle curves and by fitting with Eq. (6) (or by comparing with Fig. 3), one can extract q_s and therefore gain access to the relaxation at the boundary, even if it occurs on a much shorter length scale than the spatial resolution of $s_z(x)$. Finally, for an inhomogeneous sample, a local probe of the spin lifetime is desirable. While it is now clear that spin diffusion can make such a measurement difficult in the steady state, one could instead use a time-resolved (pump-probe) measurement to determine $\tau_s(x)$.

Instead of extracting the parameters of Eqs. (1) and (2) by fitting to Eq. (6), one can find some parameters more directly as follows. First, note that for $B=0$, one can extract the decay length $L_s^z = \sqrt{D\tau_z}$ from $s_z(x)$. Next, the width of the Hanle curve contains information about spin relaxation, and we access it via the curvature at the origin, $c(x) = (\partial^2 s_z / \partial B^2) / s_z|_{B=0}$. (The normalization of c eliminates effects of a spatially dependent detection sensitivity on s_z . Also, when fitting experimental data, it is presumably more accurate to fit the curvature on many data points instead of taking the discretized derivative.) Since the Hanle curve becomes narrower when moving away from the boundary, the curvature increases and from Eq. (6), we find

$$\frac{1}{c} \frac{\partial c}{\partial x} \Big|_{x=0} = \frac{1}{L_s^z} + q_s, \quad (10)$$

which does not explicitly depend on α or g^* . Because L_s^z can be determined independently, Eq. (10) provides a convenient way to access the spin relaxation q_s at the boundary.

Furthermore, note that at finite distances x , the Hanle curve can develop “side lobes,” where s_z changes sign, see Fig. 1. This is a well-known effect and such side lobes were detected electrically in Johnson-Silsbee geometries for a fixed injector-detector spacing x .^{25,26} Additionally, in the re-

gime $\tau_{xy} \gg \tau_z$ and for a fixed x , the polarization at finite fields can have a larger magnitude (but opposite sign) than the main peak at zero fields, which can be understood as follows. In the absence of spin precession (main peak), the spins will relax rapidly with rate τ_z^{-1} . However, the precessing spins corresponding to the side lobes relax with a lower average rate and thus contribute with a larger signal, effectively filtering spins that have precessed by an angle of π .

In addition to the extrinsic spin-orbit interaction, leading to the spin Hall effect considered above, there is also intrinsic spin-orbit interaction that couples to the spin as an effective field $\mathbf{b}(\mathbf{k})$, depending on the wave vector \mathbf{k} . In Eq. (1), we do not take this field into account explicitly; however, it does contribute to the spin relaxation rate τ_s^{-1} . Also, this field can lead to additional spin polarization induced by the electric field—for example, for a two-dimensional system with Rashba spin-orbit interaction, this polarization is along the x axis;^{27–33} however, it is not relevant in our discussion of s_z , since s_x does not couple to s_z or s_y in Eq. (1). In a naive model, one can understand this polarization as arising from the field $\mathbf{b}_{\text{dr}} = \langle \mathbf{b}(\mathbf{k}) \rangle$ averaged over all carriers, which drift in the electric field with a finite $\langle \mathbf{k} \rangle$. For Rashba spin-orbit interaction, \mathbf{b}_{dr} is in plane and perpendicular to \mathbf{E} , i.e., in our case $\mathbf{b}_{\text{dr}} \parallel \mathbf{B}$.

In addition to the s_x polarization, \mathbf{b}_{dr} contributes as a spin precession term in the Bloch equation. Because it is parallel to \mathbf{B} , its contribution can be absorbed into ω_L and it leads to a shifted Hanle curve $s_z(B)$ with the maximum moved away from $B=0$. Experimentally, the expected shift of the Hanle curve $s_z(B)$ was reported for strained three-dimensional n -GaAs systems (where a spin-orbit coupling with the same form as the Rashba term is present³⁴), while for unstrained samples one sees that $\mathbf{b}_{\text{dr}}=0$ due to the cubic symmetry and there is no shift.⁴ Note that this naive model can break down for more general transport mechanisms,³³ which can lead to spin generation along $\mathbf{b}_{\text{dr}} \times \mathbf{B}$, but this expression vanishes in our configuration.

Furthermore, for Rashba spin-orbit interaction, there are additional precession terms around the \hat{y} axis that arise when

spins diffuse away from the edge.^{15,35–37} This would induce oscillations in $s_z(x)$ in addition to the one shown in Fig. 1(d), and the combined effect can lead to larger oscillation amplitudes. Since the precession length is on the order of L_s in both cases, strictly speaking, our model [Eq. (1)] does not apply to a system with Rashba spin-orbit interaction; however, no such k -linear intrinsic spin-orbit terms are present for a three-dimensional system with cubic symmetry, which applies to the experiments of Ref. 4 on unstrained samples. Finally, for two-dimensional systems, it was argued that the Rashba spin-orbit interaction can change the magnitude of extrinsic spin currents^{38,39} and would thus change the magnitude of the Hanle curves. For these systems, also the importance of the intrinsic spin-orbit interaction on the boundary conditions was studied,^{17,18} measuring the spatial dependence of the Hanle curves and using a property analogous to Eq. (10) can be used to test these predictions.

IV. CONCLUSIONS

In conclusion, we have found that in systems where spins are generated at the boundary, the magnetic field dependence of the spin polarization (Hanle curve) becomes spatially dependent even if the spin relaxation rate τ_s^{-1} is spatially homogeneous. This leads to a reduction of the apparent spin lifetimes $\tilde{\tau}_s$ near the edges of a sample exhibiting the spin Hall effect, as was recently observed experimentally.⁴ We have provided an intuitive picture for this effect: Spins detected closer than L_s to the edge were, on average, generated within a time less than τ_s and relatively large magnetic fields would be required to suppress them, corresponding to a small $\tilde{\tau}_s$. Our description provides a method for extracting the homogeneous spin relaxation rate and it also allows us to measure spin relaxation effects at the sample boundary.

ACKNOWLEDGMENTS

We thank I. G. Finkler, B. I. Halperin, J. J. Krich, and E. I. Rashba for many useful and insightful discussions. This work was supported by NSF Grants No. DMR-05-41988 and No. PHY-01-17795.

¹*Optical Orientation*, edited by F. Meier and B. P. Zakharchenya (North-Holland, Amsterdam, 1984), and references therein.

²S. A. Wolf, D. D. Awschalom, R. A. Buhrman, J. M. Daughton, S. von Molnár, M. L. Roukes, A. Y. Chtchelkanova, and D. M. Treger, *Science* **294**, 1488 (2001).

³*Semiconductor Spintronics and Quantum Computation*, edited by D. D. Awschalom, D. Loss, and N. Samarth, Series on Nanoscience and Technology (Springer, Berlin, 2002).

⁴Y. K. Kato, R. C. Myers, A. C. Gossard, and D. D. Awschalom, *Science* **306**, 1910 (2004).

⁵M. I. D'yakonov and V. I. Perel', *JETP Lett.* **13**, 467 (1971).

⁶J. E. Hirsch, *Phys. Rev. Lett.* **83**, 1834 (1999).

⁷H.-A. Engel, B. I. Halperin, and E. I. Rashba, *Phys. Rev. Lett.* **95**, 166605 (2005).

⁸W.-K. Tse and S. Das Sarma, *Phys. Rev. Lett.* **96**, 056601 (2006).

⁹S. A. Crooker, M. Furis, X. Lou, C. Adelman, D. L. Smith, C. J.

Palmström, and P. A. Crowell, *Science* **309**, 2191 (2005).

¹⁰Y. K. Kato, R. C. Myers, A. C. Gossard, and D. D. Awschalom, *Appl. Phys. Lett.* **87**, 022503 (2005).

¹¹V. Sih, W. H. Lau, R. C. Myers, V. R. Horowitz, A. C. Gossard, and D. D. Awschalom, *Phys. Rev. Lett.* **97**, 096605 (2006).

¹²I. G. Finkler, H.-A. Engel, E. I. Rashba, and B. I. Halperin, *Phys. Rev. B* **75**, 241202(R) (2007).

¹³M. I. D'yakonov and V. I. Perel', *Sov. Phys. Solid State* **13**, 3023 (1972).

¹⁴M. I. D'yakonov and V. Y. Kachorovskii, *Sov. Phys. Semicond.* **20**, 110 (1986).

¹⁵A. A. Burkov, A. S. Núñez, and A. H. MacDonald, *Phys. Rev. B* **70**, 155308 (2004).

¹⁶W. H. Lau and M. E. Flatté, *Phys. Rev. B* **72**, 161311(R) (2005).

¹⁷O. Bleibaum, *Phys. Rev. B* **74**, 113309 (2006).

¹⁸Y. Tserkovnyak, B. I. Halperin, A. A. Kovalev, and A. Brataas,

- Phys. Rev. B **76**, 085319 (2007).
- ¹⁹M. D'yakonov and V. Perel', Sov. Phys. Semicond. **10**, 208 (1976).
- ²⁰V. B. Vekua, R. I. Dzhioev, B. P. Zakharchenya, and V. G. Fleisher, Sov. Phys. Semicond. **10**, 210 (1976).
- ²¹M. Johnson and R. H. Silsbee, Phys. Rev. B **37**, 5312 (1988).
- ²²M. Johnson and R. H. Silsbee, Phys. Rev. Lett. **55**, 1790 (1985).
- ²³N. P. Stern, S. Ghosh, G. Xiang, M. Zhu, N. Samarth, and D. D. Awschalom, Phys. Rev. Lett. **97**, 126603 (2006).
- ²⁴That a homogeneous τ_s can result in such an inhomogeneous $\tilde{\tau}_s$ was also found recently and compared to numerical simulations [N. P. Stern, D. W. Steuerman, S. Mack, A. C. Gossard, and D. D. Awschalom, Appl. Phys. Lett. **91**, 062109 (2007)].
- ²⁵F. J. Jedema, H. B. Heersche, A. T. Filip, J. J. A. Baselmans, and B. J. van Wees, Nature (London) **416**, 713 (2002).
- ²⁶S. O. Valenzuela and M. Tinkham, Nature (London) **442**, 176 (2006).
- ²⁷E. L. Ivchenko and G. Pikus, JETP Lett. **27**, 604 (1978).
- ²⁸F. T. Vas'ko and N. A. Prima, Sov. Phys. Solid State **21**, 994 (1979).
- ²⁹L. S. Levitov, Y. N. Nazarov, and G. M. Eliashberg, Sov. Phys. JETP **61**, 133 (1985).
- ³⁰V. M. Edelstein, Solid State Commun. **73**, 233 (1990).
- ³¹A. G. Aronov, Y. B. Lyanda-Geller, and G. E. Pikus, Sov. Phys. JETP **73**, 537 (1991).
- ³²B. A. Bernevig and S.-C. Zhang, Phys. Rev. B **72**, 115204 (2005).
- ³³H.-A. Engel, E. I. Rashba, and B. I. Halperin, Phys. Rev. Lett. **98**, 036602 (2007).
- ³⁴G. E. Pikus and A. N. Titkov, in *Optical Orientation*, edited by F. Meier and B. P. Zakharchenya (North-Holland, Amsterdam, 1984), Chap. 3, p. 73.
- ³⁵E. G. Mishchenko, A. V. Shytov, and B. I. Halperin, Phys. Rev. Lett. **93**, 226602 (2004).
- ³⁶I. Adagideli and G. E. W. Bauer, Phys. Rev. Lett. **95**, 256602 (2005).
- ³⁷E. I. Rashba, Physica E (Amsterdam) **34**, 31 (2006).
- ³⁸W.-K. Tse and S. Das Sarma, Phys. Rev. B **74**, 245309 (2006).
- ³⁹E. M. Hankiewicz and G. Vignale, <http://arxiv.org/abs/0707.2251>